AJNR

High-Resolution Spinal Sonography in Infants

Hooshang Kangarloo, Richard H. Gold, Michael J. Diament, Maria I. Boechat and Cynthia Barrett

This information is current as of April 17, 2024.

High-Resolution Spinal Sonography in Infants

Hooshang Kangarloo[1]
Richard H. Gold[1]
Michael J. Diament[1]
Maria I. Boechat[1]
Cynthia Barrett[2]

High-resolution, real-time sonography of the spine revealed significant anatomic details in 29 infants, including nine with congenital malformations. Transverse sections were most useful for detecting osteochondral anomalies and for evaluating the symmetry of the spinal column and its soft-tissue contents. Longitudinal sections augmented the transverse sections and provided the most detailed anatomy of the cord and spinal arteries. A normal screening sonographic examination obviates ionizing radiation and invasive procedures, while an abnormal study implies the need for further, complementary diagnostic investigations.

Incomplete posterior ossification of the immature spine permits infants with cutaneous changes suggestive of spinal dysraphism to be examined for anomalies of the spinal cord and canal by high-resolution, real-time sonography. A normal sonographic examination obviates ionizing radiation and the cost and morbidity of invasive radiologic procedures, while abnormal sonographic findings may lead to further, complementary diagnostic procedures such as computed tomography (CT). A recent report [1] evaluating spinal dysraphism emphasized the longitudinal sonographic anatomy of the lumbar cord and canal. We report our experience with longitudinal and transverse spinal sonography of the cervical, thoracic, and lumbosacral spine of infants.

Materials and Methods

During a 3 year period 27 infants 1 day to 3 months of age had spinal sonography at the UCLA Medical Center. Two of these had neurologic findings that resulted from syringohydromyelia in one case and spinal cord hematoma in the other. Of the other 25 infants, 21 were examined because of cutaneous manifestations suggestive of underlying dysraphism, two were examined because of multiple congenital anomalies, and two were studied after vertebral abnormalities were detected in radiographs of the abdomen. Before embarking on the clinical investigations, sonograms of two infant cadavers were correlated with spinal radiographs and autopsy findings.

The examinations were performed with a high-resolution, real-time Picker Microview scanner using a 10-MHz transducer housed in a self-contained water bath. All patients and cadavers were examined in the prone position, with both transverse and longitudinal freeze-frame images recorded on x-ray or Polaroid film by a multiformat camera. Examination of the cervical spine was accomplished by placing the chest on a pillow and allowing the head to flex downward.

Results

The two cadavers and 18 of the 27 patients manifested normal findings, with the transverse sonograms providing the most detailed anatomy of the ossified spinal column. The vertebral bodies were easily identifiable, with incompletely ossified and bilaterally symmetric posterolateral elements (fig. 1). Although the contents of
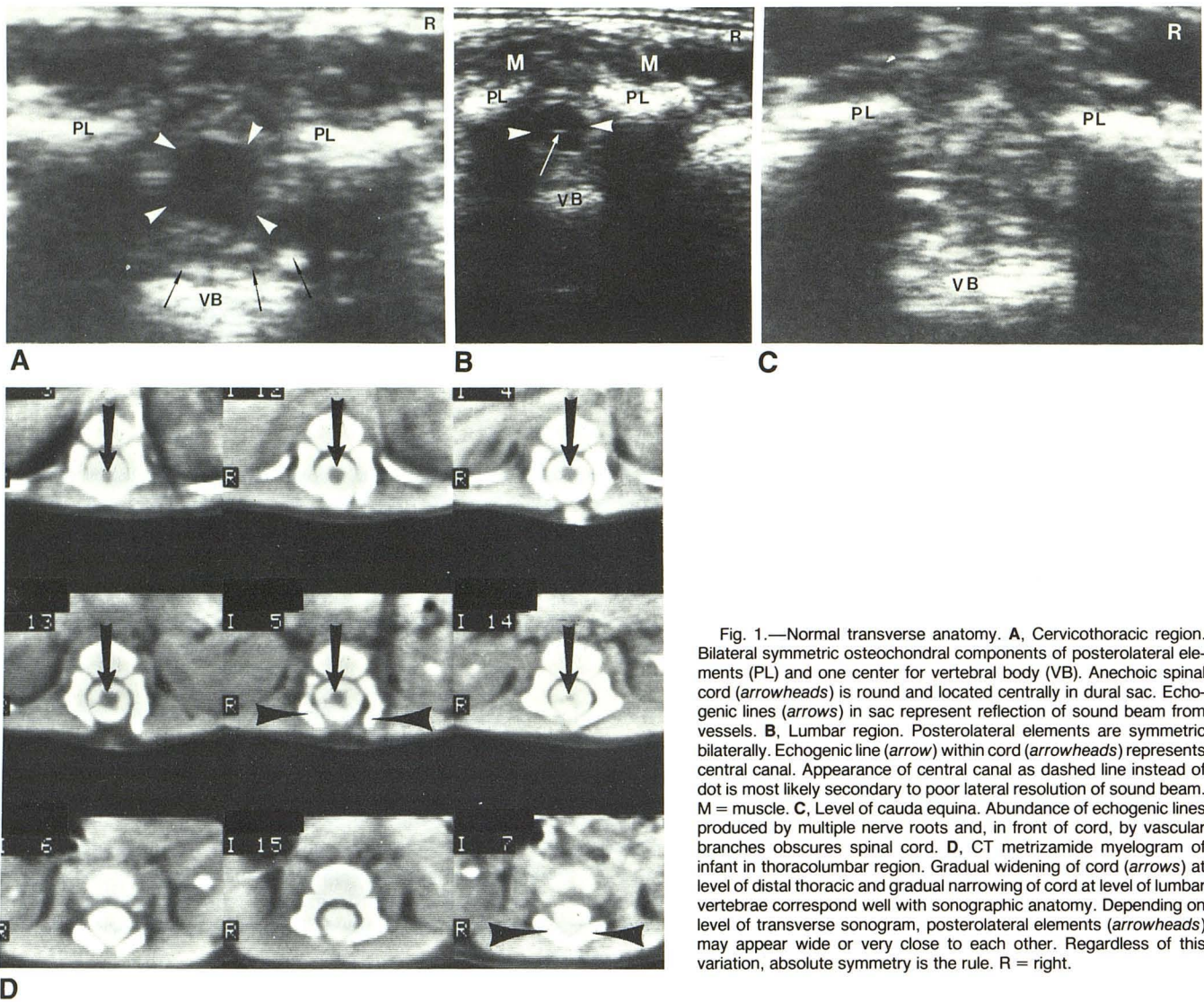
Fig. 1.—Normal transverse anatomy. **A**, Cervicothoracic region. Bilateral symmetric osteochondral components of posterolateral elements (PL) and one center for vertebral body (VB). Anechoic spinal cord (*arrowheads*) is round and located centrally in dural sac. Echogenic lines (*arrows*) in sac represent reflection of sound beam from vessels. **B**, Lumbar region. Posterolateral elements are symmetric bilaterally. Echogenic line (*arrow*) within cord (*arrowheads*) represents central canal. Appearance of central canal as dashed line instead of dot is most likely secondary to poor lateral resolution of sound beam. M = muscle. **C**, Level of cauda equina. Abundance of echogenic lines produced by multiple nerve roots and, in front of cord, by vascular branches obscures spinal cord. **D**, CT metrizamide myelogram of infant in thoracolumbar region. Gradual widening of cord (*arrows*) at level of distal thoracic and gradual narrowing of cord at level of lumbar vertebrae correspond well with sonographic anatomy. Depending on level of transverse sonogram, posterolateral elements (*arrowheads*) may appear wide or very close to each other. Regardless of this variation, absolute symmetry is the rule. R = right.

the spinal canal were visible on transverse sonograms anatomic details of the cord and spinal arteries were augmented by the longitudinal sonograms (fig. 2).

Nine infants manifested abnormal findings, with the transverse sonograms again providing important information complementing that obtained from the longitudinal sonograms (fig. 3). The lesions were classified as cervical, cervicothoracic, thoracolumbar, lumbar, or lumbosacral (table 1).

Of the nine infants with abnormal findings, one had sonographic evidence of cervical syringohydromyelia (fig. 4), which was subsequently confirmed by CT myelography. Another, with a presumptive diagnosis of cervical cord hematoma after traumatic delivery, and sonographic findings consistent with that diagnosis, had neurologic changes implying cord damage at the cervicothoracic level. One patient had sonographic findings of widely displaced laminae at the thoracolumbar

level, an enlarged dural sac, and tethered cord, but other congenital anomalies militated against surgical intervention (fig. 3).

Two patients with sonographic features of lipomatous tissue adjacent to the filum terminale and tethered cords had the diagnosis confirmed at surgery. One patient with sonographic features of a small subcutaneous lipoma that did not appear to connect to the dural sac had a CT examination of the spine that was interpreted as normal. At surgery, however, a strand from the lipoma was found to extend to the dural sac. Even retrospectively, this extension remained undetectable by sonography.

One patient with sonographic evidence of a sinus tract extending from a skin dimple overlying the sacrum toward the dural sac, and which admitted a 3 French catheter to a depth of 1 cm, had no further evaluation because a connection
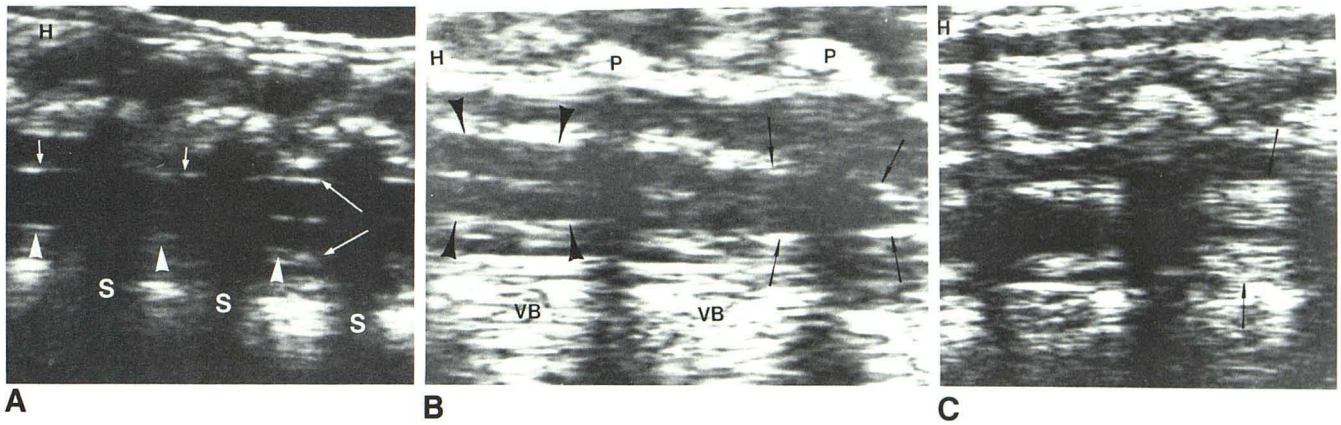
A

B

C

Fig. 2.—Longitudinal anatomy. **A**, Thoracic region. Spinal cord is centrally located within dural sac. Distally, cord widens (*long arrows*) to form conus medullaris. Anterior spinal artery is prominent at this level and visible as pulsatile structure anterior to cord (*arrowheads*). Posterior spinal artery is more difficult to visualize. *Short arrows* show possible location of posterior spinal artery. Posterior elements of vertebral column cause anterior shadowing (S). **B**, Cau-

date part of conus medullaris (*arrows*) where cord ends in filum terminale. *Arrowheads* show more cephalad part of cord with clearly visible central canal. Posterior elements (P) cause anterior shadowing. VB = vertebral body. **C**, Level of cauda equina where multiple nerve roots (*arrows*) are visible. H = head.
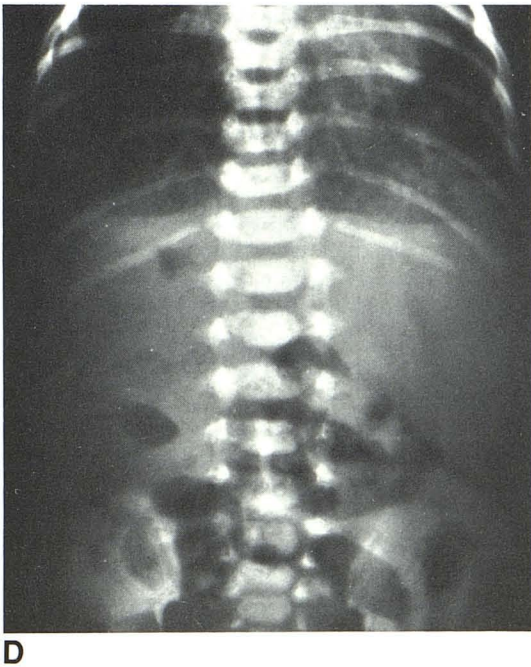

A

B

C

D
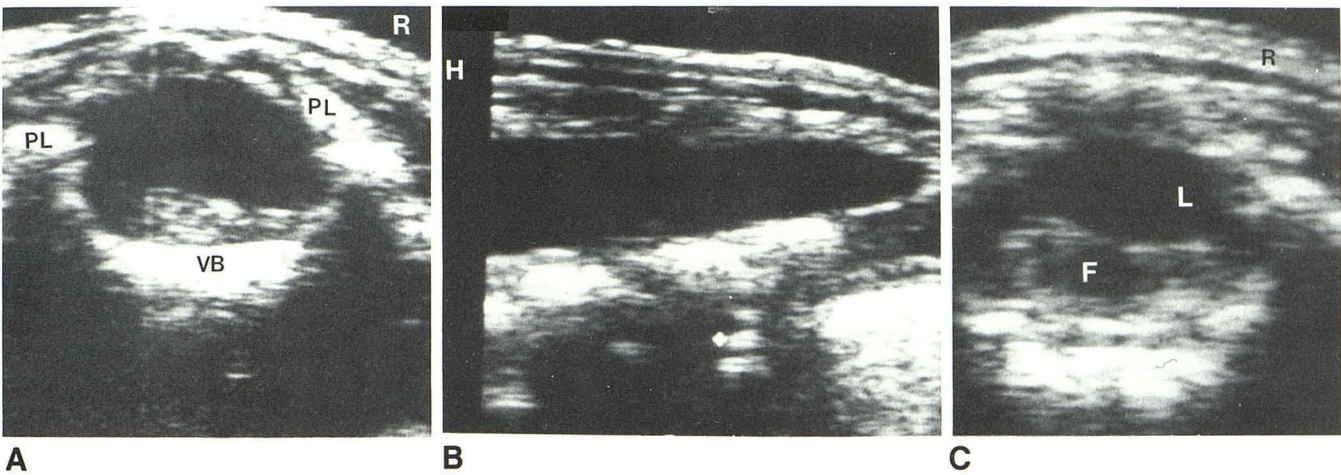
Fig. 3.—Occult spinal dysraphism. **A**, Transverse sonogram at level of L3–L4 demonstrates widely displaced and asymmetric posterolateral elements (PL). Dural sac is too wide. VB = vertebral body. **B**, Longitudinal sonogram at lumbosacral level of same patient showing widening dural sac. **C**, Transverse sonogram at level of filum terminale (F), which is thickened with posterior lipomatous tissue (L). **D**, Radiograph shows cardiomegaly, hyperaerated lungs, and abnormal bowel gas pattern—all from multiple congenital anomalies. At lumbar level, interpedicular distance appears wider than usual. R = right; H = head.

TABLE 1: **Abnormal Spinal Sonograms**

Location: No. of Cases	Abnormality	Most Useful Projection	Follow-up Confirmatory Examination
Cervical:			
1	Syringohydromyelia	Transverse and longitudinal	CT myelography
Cervicothoracic:			
1	Hematoma of cord	Longitudinal	Neurologic findings
Thoracolumbar:			
1	Wide laminae Enlarged dural sac	Transverse Transverse and longitudinal	. . .
	Tethered cord	Longitudinal	
Lumbar:			
2	Lipomatous tissue adjacent to filum terminale	Transverse and longitudinal	Surgery
	Tethered cord	Longitudinal	
2	Hemivertebrae	Transverse	Spinal radiography
Lumbosacral:			
1	Subcutaneous lipoma	Transverse	Surgery
1	Sinus tract	Transverse	. . .

between the tract and dural sac could not be found, and the neurologic examination was within normal limits. Two patients had lumbar hemivertebrae, but no other abnormalities.

Discussion

The CT and radiographic anatomy of the spine and spinal cord in infants has been well established [2–4]. High-resolution sonography can also provide significant anatomic and pathologic information about these structures [1, 5]. Sonographic anatomy, however, is different from that shown by CT because of intrinsic differences between the two imaging methods. Real-time sonography reveals not only the nonradiopaque parts of the spinal column such as cartilage, spinal cord, subarachnoid space, and nerve roots; but, more importantly, it discloses cord movements and vascular pulsations and permits rapid visualization of suspected pathology in transverse and longitudinal sections. This, in turn, provides a three-dimensional understanding of spinal anatomy and pathology.

During growth, the anatomy of the spine and the size of the spinal canal relative to that of the vertebral bodies is subject to rapid change [6]. In infants, unlike adults, the spine is relatively straight from occiput to coccyx. Thus, the cord is centrally located from the cervical to the lumbar regions. Once the child is able to sit, a normal thoracic kyphosis develops,

and, in the thoracic spine, the cord comes to lie closer to the anterior than to the posterior wall of the canal [7].

Osteochondral components of the vertebral bodies and posterolateral elements are best visualized on transverse sonograms. The vertebral bodies and posterior elements at the site of suspected spinal dysraphism should be compared with sections above and below that site. The bodies are visible at all levels, and the posterolateral elements are consistently visible with bilaterally symmetric obliquity from their dorsal to ventral aspects (fig. 1). Absolute symmetry of the posterolateral elements is the rule, regardless of age-dependent variations of spinal anatomy.

The spinal cord is anechoic, but its central canal is echogenic, most likely the result of imaging the anterior and posterior aspects of the wall of the central canal as a single structure because they are too closely spaced to be resolved (fig. 1B). The subarachnoid space is anechoic, but contains echogenic structures, probably representing the nerve roots and vascular branches. In infants, unlike adults, the transverse diameter of the canal is wider than the vertebral bodies at all levels of the spine [7]. Moreover, the infant cord is round in the cervical region, becoming oval in the distal thoracic region. At the level of T10–T11, the cord widens into a bulbous conus medullaris, while at L1–L2, the conus narrows to form the filum terminale [7]. More distally, the nerve roots forming the cauda equina are visible as multiple echogenic linear structures (fig. 1C). The filum terminale in infants may begin as low as L2–L3 without being of pathologic significance. The spinal cord and the level of filum terminale are shown most clearly on longitudinal sonograms (fig. 2). The anterior spinal artery is prominent near the conus, and its rapid pulsations allow it to be easily identified by high-resolution, real-time sonography (fig. 2A).

The term spinal dysraphism includes a wide variety of abnormalities that may be occult or that may be associated with hairy or pigmented nevi, dermal sinus, lipoma, meningocele, or myelomeningocele [8]. Abnormalities of the posterior neural arches range from spina bifida, with sonographically visible bilaterally asymmetric posterolateral elements, to widely separated vertebral components. Although there is no direct correlation between the severity of the vertebral anomalies and underlying neural abnormalities, detection of neural arch anomalies requires sonography with a high resolving capacity. Abnormalities of the spinal cord and dural sac may be as minor as an increase in the width of the sac or a thickened filum terminale with tethered cord (fig. 3), or as extensive as overt meningocele, myelomeningocele, diastematomyelia, or syringohydromyelia [9–11]. Other associated abnormalities result from overgrowth of sequestered fetal tissue, and include fatty infiltration of the cord, dermoid, lipoma, and teratoma.

The tethered cord syndrome [12] is present in more than one-half of patients with spinal dysraphism and is manifested by a thickened filum terminale in an excessively caudal location in association with decreased pulsatile motion of the spinal cord. In more severe cases the cord itself may extend too caudally (low-cord syndrome). Visualization of the central canal of the cord may be useful in distinguishing it from a thickened filum terminale.
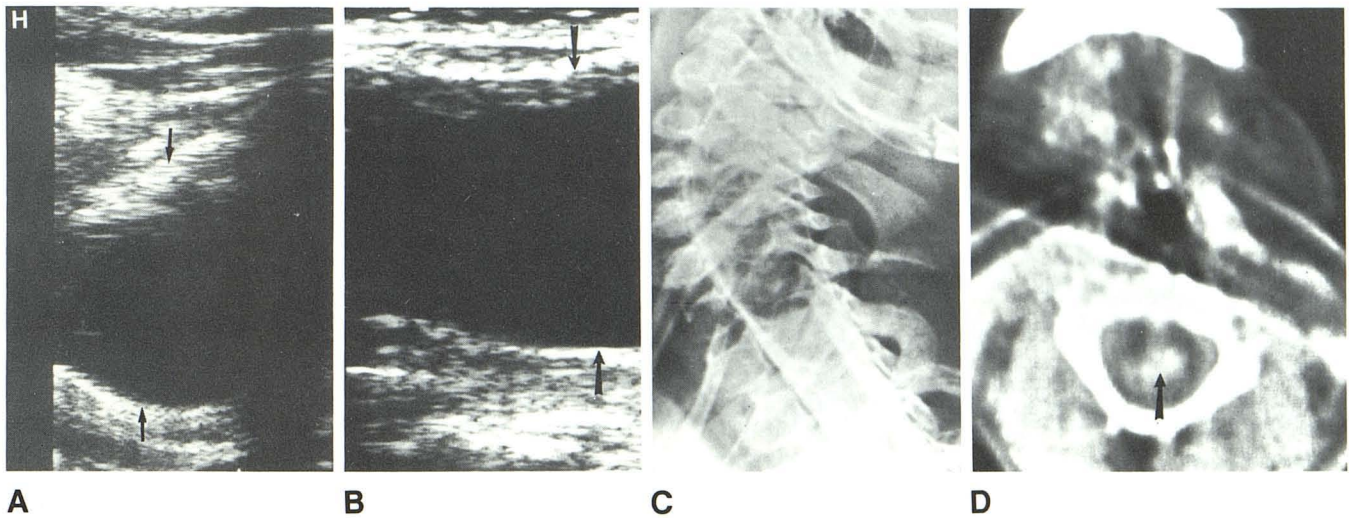
Fig. 4.—Syringohydromyelia. **A** and **B**, Longitudinal sonograms of cervical region reveal strikingly widened dural sac (*arrows*) with no sign of cord. **C**, Myelogram shows marked widening of canal and cord in cervical region. **D**, CT scan after myelogram shows central accumulation of contrast (*arrow*). H = head.

REFERENCES

1. Scheible W, James HE, Leopold GR, Hilton SVW. Occult spinal dysraphism in infants: screening with high-resolution real-time ultrasound. *Radiology* **1983**;146:743–746
2. Coin G, Keranen VJ, Pennink M, Ahmad WD. Computerized tomography of the spine and its contents. *Neuroradiology* **1978**;16:271–272
3. Lee BCP, Kazam E, Newman AD. Computed tomography of the spine and spinal cord. *Radiology* **1978**;128:95–102
4. Resjo IM, Harwood-Nash DC, Fitz CR, Chung S. Normal cord in infants and children examined with computed tomographic metrizamide myelography. *Radiology* **1979**;130:691–696
5. Miller JH, Reid BS, Kemberling CR. Utilization of ultrasound in the evaluation of spinal dysraphism in children. *Radiology* **1982**;143:737–740
6. Nordqvist L. The sagittal diameter of the spinal cord and subarachnoid space in different age groups. A roentgenographic postmortem study. *Acta Radiol* (Stockh) **1964**;227:1–6
7. Pettersson H, Harwood-Nash DCF. *CT and myelography of the spine and cord. Techniques, anatomy and pathology in children.* Berlin: Springer-Verlag, **1982**:23–37
8. Lichtenstein BW. "Spinal dysraphism." Spina bifida and myelodysplasia. *Arch Neurol Psychiatr* **1940**;44:792–810
9. Resjo IM, Harwood-Nash DC, Fitz CR, Chuang S. Computed tomographic metrizamide myelography in spinal dysraphism in infants and children. *J Comput Assist Tomogr* **1978**;2:549–558
10. McRae DL, Standen J. Roentgenologic findings in syringomelia and hydromyelia. *AJR* **1966**;98:695–703
11. Scotti G, Musgrave MA, Harwood-Nash DC, Fitz CR, Chuang SH. Diastematomyelia in children: metrizamide and CT metrizamide myelography. *AJNR* **1980**;1:403–410, *AJR* **1980**;135: 1225–1232
12. Fitz CR, Harwood-Nash DC. The tethered conus. *AJR* **1975**;125:515–523